Hybrid WiFi/UWB, Cooperative Localization using Particle Filter

Nader Bargshady, Kaveh Pahlavan
Center for Wireless Information Network Studies
Worcester Polytechnic Institute
Worcester, MA, 01609, USA
Email: {nbargsha, kaveh}@wpi.edu

Nayef A. Alsindi
Etisalat BT Innovation Center (EBTIC)
Khalifa University of Science Technology and Research (KUSTAR)
Abu Dhabi, UAE
Email: nayef.alsindi@kustar.ac.ae

***Abstract*—Indoor navigation using RF signals has attracted tremendous attention in the recent years. However, indoor localization using RF signaling is very challenging and does not provide adequate precision for many applications. In this paper we use Particle Filter (PF) to integrate the Received Signal Strength (RSS) of WiFi and the Time Of Arrival (TOA) of UWB RF signaling for precise cooperative localization in indoor environment. The choice for PF is due to non-linear and Non-Gaussian channel models for RF localization algorithm. We use channel models for the RSS of WiFi and the TOA of UWB. The performance of the PF results are evaluated in a typical indoor scenario and are compared with the Cramér-Rao-Lower-Bound (CRLB) for Hybrid (UWB & WiFi) in Cooperative (COOP) and non-Cooperative (NCOOP) modes.**

***Index Terms*—UWB, TOA, WiFi, RSS, PF, MO, FA, CRLB, COOP, NCOOP, LOS, NLOS**

I. Introduction

Localization is one of the most crucial components for carrying out successful cooperative moving objects operations in civilian and medical domains. Civilian applications include the removal and handling of unwanted hazardous materials. Another is emergency responder operations. Examples include search and rescue of civilians inside burning structures where access by fire-fighters is limited and/or too dangerous. In aforementioned scenarios the ability to obtain accurate location information for the cooperating moving objects is of utmost importance for the effectiveness of the operation.

When these applications are concerned, there are several ways to perform localization. To compare the performance of these alternative techniques, CRLB is used as the benchmark. The CRLB results for the Time Of Arrival (TOA) of UWB and the Received Signal Strength (RSS) of WiFi were investigated and anlayzed in [1] and [2] respectively. In [3], we showed that Cooperative localization was very effective in performance enhancement when using RSS or UWB or both (Hybrid) signaling. In [3], the CRLB was calculated for the Hybrid and Cooperative localization using a mix of WiFi and UWB signaling. It was shown that the TOA-based UWB signaling results in more precise localization than RSS-based WiFi. However, the WiFi infrastructure is more readily available and widespread over UWB infrastructure making it more commercially viable.

In dynamic tracking applications, adaptive filters are used to improve the localization accuracy by reducing the estimation error. Particle filters have shown to be very effective and widely used for these purposes [4]. Various applications of PF in Wireless Sensor Networks were discussed in [5].

In this paper, we propose a novel Hybrid WiFi-UWB cooperative localization using Particle Filter. There are different issues in implementing particle filters, one important implementation issue is the Resampling. Our implementation of the PF is similar to Systematic Resampling approach discussed in [6]. Due to the complex nature of radio propagation, employing Hybrid and Cooperative localization methods has become increasingly attractive. Accuracy of methods such as TOA and RSS are highly susceptible to non-linear, non-Gaussian channel models in indoor environments. The Particle Filter is chosen for this work to deal with such an environment. We analyze the performance of the Particle Filter versus CRLB by using the theoretical, IEEE 802.11 channel model for RSS and the empirical one for UWB ranging error as presented in [7]. For our performance platform, we leverage off the previous findings in [3], where we used eight fixed anchors (FAs) along with three moving objects (MOs). The performance of the PF results are evaluated in a typical indoor scenario and are compared with CRLB result for the Hybrid (UWB & WiFi), in Cooperative (COOP) and non-Cooperative (NCOOP) modes.

The rest of the paper is organized as follows: In section II, we define distance measurement error, describe power calculation based on 802.11 RSS model, use the power for TOA-based link error variance selection according to empirical model from [7] and calculate RSS-based link error variance from [2]. Section III, a brief CRLB formulation is outlined. Section IV, we formulate the Particle Filter steps based on Bayesian method. Section V, we describe the simulation environment, the definition for Hybrid, Cooperative, non-Cooperative and various configurations. Section VI, the results of our research are analyzed in detail. Section VII, we show the conclusion of our research and findings. October 2, 2014

II. Channel models and Ranging error variances

In this section, we define ranging error, power calculation and channel models for ranging error variances of UWB

TOA-based and WiFi RSS-based ranging techniques. First, we describe the distance definition and its error, Distance Measurement Error (DME). We then describe the IEEE 802.11 channel model for power (RSS) calculation. The calculated power is used to select link error variance for UWB TOA-based ranging technique according to empirical data [7]. Lastly, we describe the theoretical ranging error variance of RSS-based ranging technique [2].

A. Ranging Error

Let us assume there are M moving objects (MOs) and A fixed anchor points (FAs), the 2-dimensional coordinates for M MOs, L_M and A FAs, L_A are given by:

$$\begin{aligned} L_M &= [(x_1, y_1), ..., (x_M, y_M)]^T \\ L_A &= [(x_{f1}, y_{f1}), ..., (x_{fA}, y_{fA})]^T \end{aligned} \tag{1}$$

where (x_i , y_i); i = 1, ... ,M denotes the x-y coordinate of M moving objects. and (x_{fj} , y_{fj}); j = 1, ... ,A denotes the x-y coordinate of A fixed anchors.

For pairs of MO-to-MO or MO-to-FA within the communication range, a measurement of Euclidean distance $d_{ij} = \sqrt{(x_i - x_j)^2 + (y_i - y_j)^2}$ can be obtained using TOA-UWB or RSS-WiFi ranging techniques. The ranging techniques are susceptible to noise variation of the channel models hence, the Distance Measurement Error (DME), ϵ_{ij} is defined as:

$$\epsilon_{ij} = \hat{d_{ij}} - d_{ij} \tag{2}$$

where $\hat{d_{ij}}$ is the estimate of the distance between pairs. ϵ_{ij} will vary between the pairs according to selected link error discussed in subsections II-C and II-D. The intent is to find the location of moving object with respect to fixed Anchor (FA) locations and compare it with actual location.

We are only analyzing the ranging error variance resulting from distance estimate, $\hat{d_{ij}}$ using the non-linear, non-Gaussian channel model and Particle Filter estimator. We make no assumptions of the speed and the trajectory complexity of the MOs in our analysis.

B. Power calculation to select ranging error variance for TOA-based technique

The Received Signal Strength (RSS) for a link between a pair is calculated based on the distance, d_{ij} by:

$$RSS(d_{ij}) = RSS_{1m} - 10\alpha \cdot log(d_{ij}) + \chi \tag{3}$$

Where RSS_{1m} is the received signal strength at a reference distance of $1m$, α is the path loss gradient and χ is the lognormal shadow fading with zero mean and variance σ_χ^2. The values of α, σ_χ for LOS and NLOS conditions are listed in different rows in table I.

C. TOA-based ranging error variance

The variance, $\sigma^2_{\epsilon_{UWB}}$ of Distance Measurement Error in (2) for UWB-based link is determined by comparing the value of calculated power in (3) with tabulated range in Table II.

The thresholds and variances defined in table II are based on Empirical data [7]. There is more general discussion of Distance Measurement Error in [8].

D. RSS-based ranging error variance

The variance of Distance Measurement Error in (2) for WiFi-based link is determined theoretically based on derivation outlined in [2]. The values of α, σ_χ for LOS and NLOS conditions are listed in different rows of table I.

$$\sigma^2_{\epsilon_{WiFi}} \geq (\frac{ln10}{10})^2 \cdot \frac{\sigma_\chi^2}{\alpha^2} \cdot d_{ij}^2 \tag{4}$$

III. Calculation of CRLB for Performance

To calculate the CRLB, we need to calculate the variance(s) of Distance Measurement Error(s) (DME) for all the links among the MOs and the MOs-to-FAs points. The CRLB provides a lower bound on the error covariance matrix for an unbiased estimate of L_M. For a given estimate of the MOs, $\hat{L_M}$ and Gaussian range measurement R, the Fisher Information Matrix (FIM) can be represented by [9]:

$$J(L_M) = E[\bigtriangledown_{L_M} ln f_R(r; L_M)][\bigtriangledown_{L_M} ln f_R(r; L_M)]^T \tag{5}$$

where $f_R(r; L_M)$ is the joint Gaussian PDF given by:

$$f_R(r; L_M) = \frac{1}{(2\pi)^K |\sum|^{\frac{1}{2}}} \times E \tag{6}$$

where

$$E = exp\left\{-\frac{1}{2}[r - \mu(L_M)]^T \sum^{-1} [r - \mu(L_M)]\right\} \tag{7}$$

and $\mu(L_M)$ is the vector of the actual distances between the nodes corresponding to available K measurements. FIM for the specific PDF in (6) can be written as:

$$J(L_M) = [G(L_M)]^T \sum^{-1} [G(L_M)] \tag{8}$$

where

$$G(L_M)^T = \begin{pmatrix} cos\phi_1 & cos\phi_2 & ... & cos\phi_k \\ sin\phi_1 & sin\phi_1 & ... & sin\phi_k \end{pmatrix} \tag{9}$$

$$\sum = diag(\lambda_1 \quad \lambda_2 \quad ... \quad \lambda_k) \tag{10}$$

ϕ_i representing the angle between the nodes from ith measurement. and λ_i is the variance of range estimate from the

TABLE I
PATH LOSS GRADIENT & SHADOW FADING STD

	RSS_{1m} (dBm)	UWB		WiFi	
		α	σ_χ	α	σ_χ
LOS	-42	2.0	6.8	2.0	8.0
NLOS	-42	5.6	8.5	3.5	8.0

TABLE II
TOA-BASED EMPIRICAL DATA

	Power (dBm)		$\sigma^2_{\epsilon_{UWB}}$
$-\infty <$	$RSS(d_{ij})$	$\leq$ -80	$(0.12)^2$
-80 $<$	$RSS(d_{ij})$	$\leq$ -100	$(0.3)^2$
-100 $<$	$RSS(d_{ij})$	$< +\infty$	$(1.4)^2$

ith measurement. The variance calculation are discussed in subsections II-C and II-D that are used to replace λ_i based on a given configuration shown in Table III. The CRLB is given by:

$$CRLB = [J(L_M)]^{-1} \tag{11}$$

And, the Root-Mean-Square-Error, RMSE is given by:

$$RMSE = \sqrt{trace(CRLB)} \tag{12}$$

IV. Particle Filter Formulation

The Particle Filter is chosen for this work due to nature of non-closed form, non-linear and non-Gaussian channel models for RF localization algorithm. The PF state is defined by uniformly Random X or Y movement of moving object (MO). The PF observation is modeled based on empirical data for UWB-TOA and theoretical approach for WiFi-RSS ranging. The distance of the moving object is obtained with respect to fixed anchors (FA) and other moving objects in cooperative mode. In the following subsections we describe the assumptions for PF setup, derive PF recursion step, outline the PF implementation and discuss the simulation environment.

A. PF setup

The notations moving forward and the assumptions for Bayesian recursion are defined here. First, the notations used are, $\mathbb{P}$ denoting probability, p denoting the index of a particle, nP denoting number of particles and $nSMP$ denoting number of samples (movement). Second, the PF State (or movement) and Observation (or measurement) are defined as d_p and RSS_p respectively. Lastly, given the random nature of MO movements and independent Observations we assume that the current location of MO depends only on the previous location hence, a Markov Process for the MOs movement (PF State),

$$\mathbb{P}(d_p/d_{0:p-1}) = \mathbb{P}(d_p/d_{p-1}) \tag{13}$$

and, the current PF observation, RSS_p depends only on the current PF state d_p, therefore:

$$\mathbb{P}(RSS_p/d_{0:p}, RSS_{0:p-1}) = \mathbb{P}(RSS_p/d_p) \tag{14}$$

B. PF Recursion Step

Leveraging off of the assumptions highlighted in subsection IV-A, we start with Bayesian rule and skip detail derivation for future paper, we arrive at the recursion for $Posterior$ of State given our measurements, $\mathbb{P}(d_{0:p}/RSS_{0:p})$, applying Bayes rule:

$$\mathbb{P}(d_{0:p}/RSS_{0:p}) = \frac{\mathbb{P}(RSS_{0:p}/d_{0:p}) * \mathbb{P}(d_{0:p})}{\mathbb{P}(RSS_{0:p})} \tag{15}$$

Starting with Bayes rule and applying our assumptions we arrive at PF Recursion step:

$$\mathbb{P}(d_p/RSS_{0:p}) = \frac{\mathbb{P}(RSS_p/d_p)}{\mathbb{P}(RSS_p/RSS_{0:p-1})} * \mathbb{P}(d_p/RSS_{0:p-1}) \tag{16}$$

where $p = 1, 2, ..., nP$. Basically, we want to pick the most suitable next state d_p given the set of observations RSS_p. Obviously, we like to pick the most likely or highest marginal $Posterior$.

C. PF implementation

Our model for state are sample points shown on Fig. 1. The Observation model is defined in (3). However, this is just a Power measurement and there are other transformations due to LOS, NLOS, UWB, WiFi conditioning in order to evaluate our Distance Measurement Error hence, link error variance.

By observing (16), it appears that the $Prior$ for the past $p-1$ observations are scaled to form the marginal $Posterior$ on the left hand side. The Scale factor can be considered as $Weight$ factor where we can recursively update by performing nP scaled version of $Prior$ to form a new $Posterior$ distribution.

$$Weight_p = \frac{\mathbb{P}(RSS_p/d_p)}{\mathbb{P}(RSS_p/RSS_{0:p-1})} \tag{17}$$

Given d_p, the numerator can be measured and the denominator does not depend on the state, d_p. For the purpose of our simulation we will use a Gaussian $Prior$ with variance σ^2_{RSS} and the mean is adjusted by the power calculated for d_p, RSS_p.

$$f_W(w_p) = \frac{1}{2\pi\sigma^2_{RSS}} exp\left\{-\frac{(RSS_{ref} - RSS_p)^2}{2\sigma^2_{RSS}}\right\} \tag{18}$$

RSS_{ref} is the power at the actual location. The state samples are also distributed in random using Gaussian with a different variance $\sigma^2_{d_p}$ prior to Observation (measurement). All the configurations outlined in Table III are simulated using the pseudo steps in Algorithm 1. Now that we got some idea of the work involved, let us evaluate some initial result for performance of PF in subsection V-A and set the stage for the intended evaluation in section VI.

Algorithm 1 PF Algorithm flow

```
if (NCoop) then                          ▷ MOs in NCoop mode
    RefPoints = 8;                       ▷ 8 Fixed Anchors
else                                     ▷ 3 Coop MOs
    RefPoints = 11;
end if
for S = 1 → nSMP do                      ▷ Objects movement
    for R = 1 → RefPoints do
        for p = 1 → nP do                ▷ Particle iterations
            a) Measurement
            b) Weight update
        end for
        1) Normalize the Weight
        2) Randomly Sample the above CDF
        3) Pick maximum likelihood sample
        4) Selection of new State, hence lowest DME
    end for
end for
```

V. Performance Analysis scenarios

In this section, we describe the simulation environment and setup in detail. The Hybrid, Cooperative, non-Cooperative are defined and various configurations are presented in tabular form.

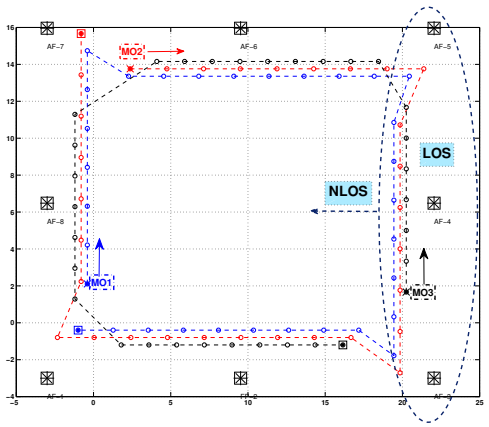

Fig. 1. **Eight Fixed Anchors** {AF1, AF2,.....,AF8} and **three moving objects** {MO1, MO2, MO3}. The objects move along the dotted lines and in the direction of arrows.

A. Simulation environment

In Fig. 1, there are eight FAs and three MOs, two moving clockwise and the third counter-clockwise. The X or Y movements are advanced according to uniformly random distribution. In this section we are evaluating the effect of number of particles nP, different variance values for State and Observation to set the stage for the intended evaluation. In Fig. 2(a), we are evaluating the effect of 8 and 16 particles ($nP = 8, 16$) for FA and MO in WiFi-enabled mode. In COOP mode, the results are very close however, in NCOOP mode the result for higher number of particle ($nP = 16$) is slightly better, from here on the evaluation is focused on $nP = 16$. In Fig. 2(b) and 2(c) the variances for State (st) and Observation (oz) are varied for COOP and NCOOP respectively. The FAs and MOs are UWB-enabled. As expected, at low variances for state and observation, both at 2 we get the best performance and conversely we get the worst when both are set to 8. The result for UWB-enabled mode is presented graphically in Figs. 2(b) and 2(c). For other scenarios (WiFi, Hybrid) are reviewed (is not included in this paper) and the results corroborates with the results shown in this paper. After this initial PF evaluation, we use the following parameters for the reset of this paper: $nP = 16$, $\sigma^2_{d_p} = 8$, & $\sigma^2_{RSS} = 8$.

B. Hybrid and Cooperative Configuration

Hybrid is when a pair (MO-to-MO or MO-to-FA) can communicate over WiFi and UWB RF signaling hence RSS-based and TOA-based ranging is applied respectively. Cooperative, refers to MOs communicating among each other in pairwise

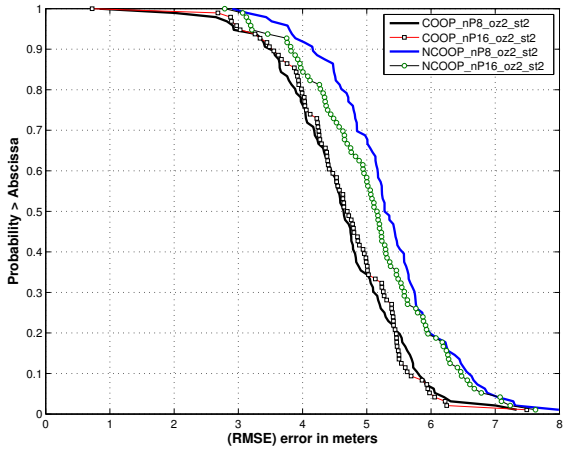

(a)

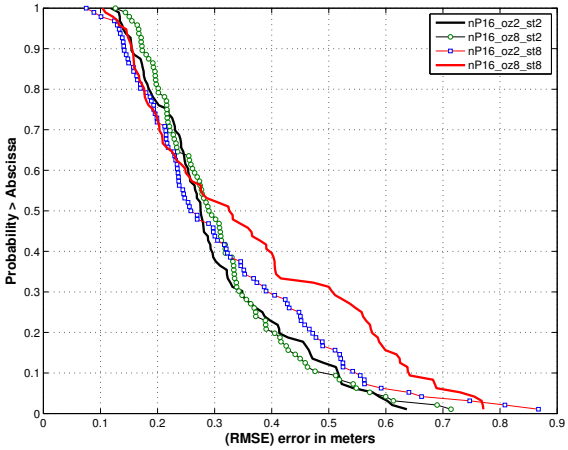

(b)

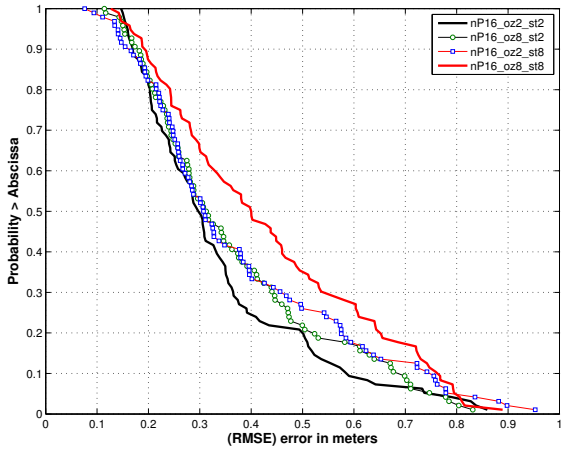

(c)

Fig. 2. **32** Samples, **8** Fixed Anchors and **3** Moving Objects.
(a) Comparison of 8 vs. 16 particles for **Coop.** and **Non-Coop.** mode.

Effect of different State and Obsevation variances on error:
(b) *COOP mode*
(c) *NCOOP mode*

TABLE III
CONFIGURATION & SELECTED RANGING TECHNIQUE

Mode	FA	MO	MO to FA	MO to MO (COOP mode)
	WiFi	WiFi	RSS-based	RSS-based
Hybrid	WiFi	UWB	RSS-based	TOA-based
	UWB	UWB	TOA-based	TOA-based
Hybrid	UWB	WiFi	TOA-based	WiFi-based

configuration. The choice of ranging technique is determined based on a given configuration shown in Table III.

TABLE IV
SIMUALTION ENVIRONMENT

Sim Parameters			PF Parameters		
$nSMP$	FAs	MOs	nP	$\sigma^2_{d_p}$	σ^2_{RSS}
32	8	3	16	8	8

VI. RESULTS AND DISCUSSION

The simulation environment for all our simulation runs moving forward is based on parameters outlined in Table IV. In this section, the Figs. 3(a), 3(b), 4(a), 4(b) and tabulated results in tables V and VI are analyzed and the performance of PF is compared to CRLB. In our review of the results we use the 50th percentile and assess the performance accordingly. Also, in each of the figures to be discussed, there is a mix of COOP and NCOOP both for PF and CRLB. The COOP and NCOOP graphs for CRLB are represented by solid Blue and Red lines respectively. In general, one can observe an improving trend stemming from Hybrid COOP mode. However, it is evident that PF does not perform as well in low error condition, for example UWB. The highlights are as follow:

$WiFi_{Anc.}, WiFi_{Obj.}$, Fig. 3(a), where FAs and MOs are WiFi-enabled hence high RMSE values, the PF tracks the CRLB both in COOP and NCOOP mode. The PF is off by 0.5 meter both in COOP and NCOOP mode with respect to the CRLB.

$Hybrid$ $(WiFi_{Anc.}, UWB_{Obj.})$, Fig. 3(b), in Hybrid mode, the MOs are UWB-enabled and FAs remain WiFi-enabled. In here, we have high RMSE values aided by low RMSE values MOs improving the overall RMSE. As a result, the PF outperfoms the CRLB when in COOP mode. In NCOOP mode, there are not much differences relative to non-Hybrid mode per Fig. 3(a). The PF performs better by 0.5 meter in COOP and is off by 0.7 meter in NCOOP mode relative to the CRLB.

$UWB_{Anc.}, UWB_{Obj.}$, Fig. 4(a), where FAs and MOs are UWB-enabled hence low RMSE values, the PF does not perform well relative to the CRLB in neither cases, COOP or NCOOP mode. The PF performs worse by 0.12 meter in COOP and 0.17 meter in NCOOP mode compared to the CRLB.

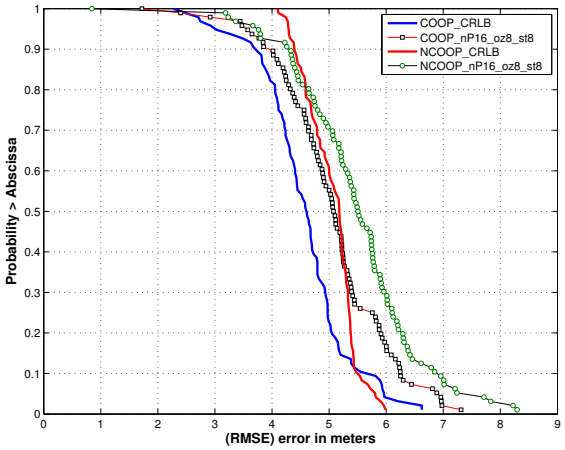

(a)

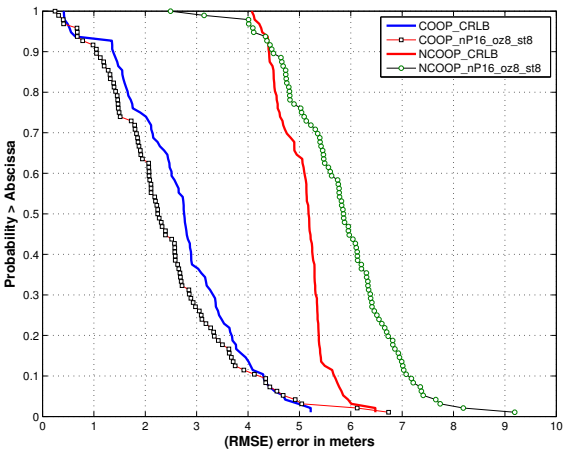

(b)

Fig. 3. *Particle filter error versus CRLB both operating in COOP and NCOOP mode using* ***WiFi*** *and* ***Hybrid*** *signaling:*
(a) $WiFi_{Anc.}$, $WiFi_{Obj.}$
(b) Hybrid($WiFi_{Anc.}$, $UWB_{Obj.}$)

$Hybrid$ $(UWB_{Anc.}, WiFi_{Obj.})$, Fig. 4(b), in Hybrid mode, the MOs are WiFi-enabled and FAs remain UWB-enabled. In here, we have low RMSE values mixed in with high RMSE values MOs which are not helping the overall RMSE as compare to 3(b). The PF performs better in COOP than

TABLE V
RMSE DEVIATION FOR PF WITH WIFI-ENABLED FAS

		Mean	STD
	WiFi-enabled MOs in Coop mode		
PF		5.0500	0.9775
CRLB		4.5540	0.8112
	WiFi-enabled MOs in NCoop mode		
PF		5.4630	1.1340
CRLB		5.0400	0.4436
	UWB-enabled MOs in Coop mode		
PF		2.4230	1.2320
CRLB		2.7010	1.1280
	UWB-enabled MOs in NCoop mode		
PF		5.8140	1.0890
CRLB		5.0670	0.4977

TABLE VI
RMSE DEVIATION FOR PF WITH UWB-ENABLED FAS

		Mean	STD
	WiFi-enabled MOs in Coop mode		
PF		0.3631	0.1955
CRLB		0.2294	0.0778
	WiFi-enabled MOs in NCoop mode		
PF		0.4334	0.2079
CRLB		0.3104	0.1661
	UWB-enabled MOs in Coop mode		
PF		0.2361	0.0956
CRLB		0.1940	0.0459
	UWB-enabled MOs in NCoop mode		
PF		0.4083	0.2283
CRLB		0.2785	0.1350

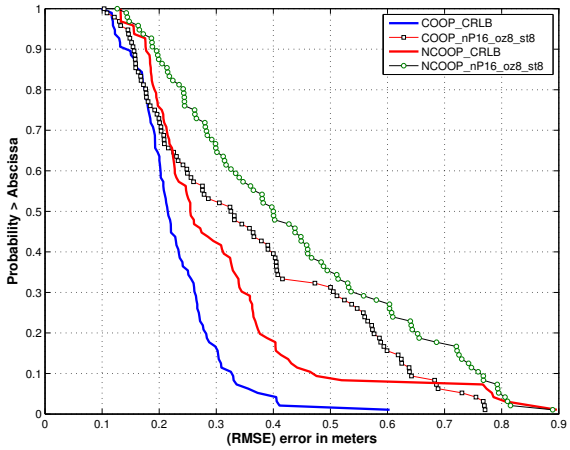

(a)

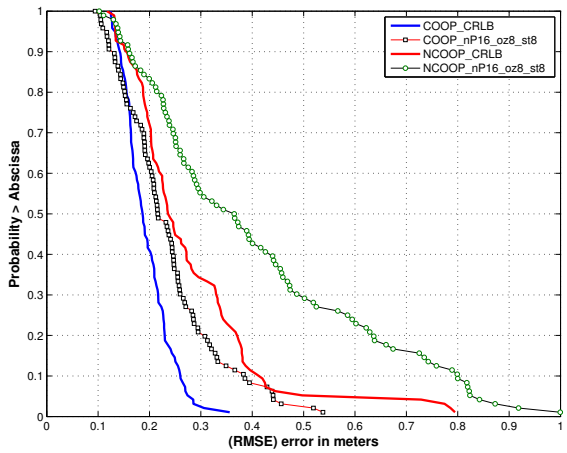

(b)

Fig. 4. *Particle filter error versus CRLB both operating in COOP and NCOOP mode using* ***UWB*** *and* ***Hybrid*** *signaling:*
(a) $UWB_{Anc.}$, $UWB_{Obj.}$
(b) Hybrid($UWB_{Anc.}$, $WiFi_{Obj.}$)

NCOOP mode. In NCOOP mode, the perfomance is similar to non-Hybrid mode result per Fig. 4(a). The PF performs worse only by 0.025 meter in COOP and worse by 0.15 meter in NCOOP mode in comparison to the CRLB.

The RMSE deviation results for the PF with parameters ($nP = 16$, $\sigma^2_{d_p} = 8$, & $\sigma^2_{RSS} = 8$) are tabulated in tables V and VI. There is higher Mean values for the PF except in Hybrid COOP where the FAs are WiFi-enabled and MOs are UWB-enabled. The STD ratio (PF/CRLB) for UWB COOP is almost the same as WiFi NCOOP. The STD for the PF is higher than the CRLB in all cases.

VII. Conclusions

In this paper, we implemented a Particle Filter for the non-linear, non-Gaussian channel models for RF localization in a Hybrid Cooperative configuration. We used UWB TOA-basedand WiFi RSS-based ranging techniques. We formulated the Bayesian approach to show the recursion step for Particle Filter implementation. We simulated and analyzed the quantitative performance of PF versus CRLB in Cooperative (COOP) and Non-Cooperative (NCOOP) both in Hybrid and non-Hybrid configurations. When the moving objects (MOs) and fixed anchors (FAs) are UWB-enabled, hence low error (RMSE) value, we showed that the PF performs poorly both in COOP and NCOOP compared to CRLB. However, in a case when moving objects and fixed anchors are all WiFi-enabled, hence high error (RMSE) value, the PF performs more closely and consistently compared to CRLB. In general, the particle filter performs much better in environment with high RMSE value in non-Hybrid configurations. We showed that in Hybrid WiFi/UWB and Cooperative configuration, the Particle Filter consistently performs well in either of low or high RMSE value environments.

Acknowledgment

The authors would like to thank our colleague, Mr. Bader Alkandari at the Center for Wireless Information Network Studies for his editorial assistance and suggestions.

References

[1] S. Gezici, Z. Tian, G. B. Giannakis, H. Kobayashi, A. F. Molisch, H. V. Poor, Z. Sahinoglu: Localization via ultra-wideband radios. IEEE Signal Processing Magazine (Special Issue on Signal Processing for Positioning and Navigation with Applications to Communications), vol. 22, issue 4, pp. 70-84, July 2005

[2] Y. Qi, H. Kobayashi: On relation among time delay and signal strength based geolocation methods. Global Telecommunications Conference, 2003. GLOBECOM '03. IEEE Volume 7, 1-5 Dec. 2003 Page(s):4079 - 4083 vol.7

[3] Bargshady, Nader, et al. "Bounds on performance of hybrid WiFi-UWB cooperative RF localization for robotic applications." Personal, Indoor and Mobile Radio Communications Workshops (PIMRC Workshops), 2010 IEEE 21st International Symposium on. IEEE, 2010.

[4] Sanjeev Arulampalam, M., Simon Maskell, Neil Gordon, and Tim Clapp. "A tutorial on particle filters for online nonlinear/non-Gaussian Bayesian tracking." Signal Processing, IEEE Transactions on 50, no. 2 (2002): 174-188.

[5] Zevedei, D., M. Jurian, and A. Scutariu. "Application of particle filter algorithms in an accurate and reliable localization and tracking of WSN's mobile devices." In Design and Technology in Electronic Packaging (SIITME), 2012 IEEE 18th International Symposium for, pp. 329-332. IEEE, 2012.

[6] Douc, Randal, and Olivier Capp. "Comparison of resampling schemes for particle filtering." In Image and Signal Processing and Analysis, 2005. ISPA 2005. Proceedings of the 4th International Symposium on, pp. 64-69. IEEE, 2005.

[7] Alsindi, Nayef, and Kaveh Pahlavan. "Cooperative localization bounds for indoor ultra-wideband wireless sensor networks. " EURASIP Journal on Advances in Signal Processing 2008 (2008): 125.

[8] B. Alavi, K. Pahlavan: Modeling of the TOA-based distance measurement error using UWB indoor radio measurements. Communications Letters, IEEE Volume 10, Issue 4, Apr 2006 Page(s):275 - 277

[9] H. L. Van Trees: Detection, Estimation, and Modulation Theory: Part I. New York: Wiley, 1968